Check for updates

Investigating the reactivity of neutral water-soluble Ru(II)–PTA carbonyls towards the model imine ligands pyridine and 2,2′-bipyridine†

Federica Battistin, [ID] ‡* Alessio Vidal, [ID] Gabriele Balducci [ID] and Enzo Alessio [ID] *

As a continuation of our strategy for preparing new Ru(II) precursors to be exploited as building blocks in the construction of metal-mediated supramolecular assemblies with improved solubility in water, here we describe the reactivity of selected neutral Ru(II)–PTA carbonyls (PTA = 1,3,5-triaza-7-phosphaadamantane) towards the model imine ligands pyridine (py) and 2,2′-bipyridine (bpy) and the preparation and characterization of several neutral and cationic water-soluble derivatives: *trans,trans,trans*-[RuCl$_2$(CO)(py)(PTA)$_2$] (**7**), *cis,cis,trans*-[RuCl$_2$(CO)$_2$(py)(PTA)] (**9**), *cis,trans*-[Ru(bpy)Cl(CO)(PTA)$_2$]Cl (**10**), *mer*-[Ru(bpy)(CO)(PTA)$_3$](Cl)$_2$ (**12**), *cis,trans*-[Ru(bpy)(CO)$_2$Cl(PTA)]Cl (**13**), *cis,trans*-[Ru(bpy)(CO)$_2$(PTA)$_2$](NO$_3$)$_2$ (**14NO$_3$**). In addition, we found that light-induced isomerization in some bpy compounds could be induced. The following species, either side-products isolated in low yield or compounds obtained exclusively in solution, were also unambiguously identified: *cis,cis,trans*-[RuCl$_2$(CO)(py)(PTA)$_2$] (**8**), *trans*-[RuCl$_2$(bpy)(CO)(PTA)] (**11**), *cis,cis*-[Ru(bpy)Cl(CO)(PTA)$_2$]Cl (**15**) and *cis,cis*-[Ru(bpy)(CO)$_2$Cl(PTA)]Cl (**16**). The X-ray structures of **7**, **11**·H$_2$O, and **12**·7H$_2$O are also reported. All compounds are new and – with few exceptions – show a good solubility in water.

Introduction

The cage-like monodentate phosphane 1,3,5-triaza-7-phosphaadamantane (PTA, Fig. 1)[1] is an amphiphilic, air-stable, neutral ligand that – besides dissolving in several organic solvents – is characterized by a high solubility in water (*ca.* 235 g L^{-1}) by virtue of H-bonding to the tertiary amine nitrogens. The coordination chemistry of PTA has been thoroughly addressed by Peruzzini and co-workers in a series of review papers.[2] PTA typically makes strong bonds with most transition metal ions through the soft P atom (PTA-κP). P-bound PTA has moderate steric demand (cone angle 103°), good σ- and π-bonding abilities and, above all, it typically imparts excellent water solubility to its complexes. For this reason PTA metal compounds have been investigated as potential anticancer drugs,[3–7] and as homogeneous catalysts in aqueous solution or in biphasic aqueous–organic conditions.[2,8–10]

In addition, PTA-κP can bind also to other metal ions through the three hard N atoms, thus acting as a bridging ligand,[2,11] and undergo N-protonation at relatively mild pH (in Ru(II) complexes PTA-κP has a pK$_a$ value of *ca.* 3),[12,13] thus altering the charge and solubility of its complexes.

In recent years we have actively investigated the chemistry of Ru(II)–PTA compounds, mainly with the aim of obtaining new precursors to be exploited as building blocks in the construction of metal-mediated conjugates and supramolecular assemblies with improved solubility in water. Ideally, such water-soluble fragments might contribute to the solubilization in aqueous media of neutral assemblies containing hydrophobic linkers (*e.g.* synthetic porphyrins). In particular, we focused on Ru–PTA–dmso and Ru–PTA–CO compounds, describing several new derivatives and finding systematic trends.[14,15] Here we

Department of Chemical and Pharmaceutical Sciences, University of Trieste, Via L. Giorgieri 1, 34127 Trieste, Italy. E-mail: alessio@units.it

‡ Now at IMDEA Nanociencia, Ciudad Universitaria de Cantoblanco, Faraday 9, 28049 Madrid, Spain. Email: federica.battistin@imdea.org
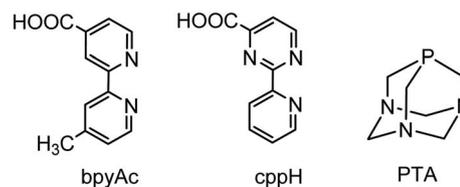
Fig. 1 Schematic structures of the chelating diimine linkers 4′-methyl-2,2′-bipyridine-4-carboxylic acid (bpyAc) and 2-(2′-pyridyl)pyrimidine-4-carboxylic acid (cppH) and 1,3,5-triaza-7-phosphaadamantane (PTA).
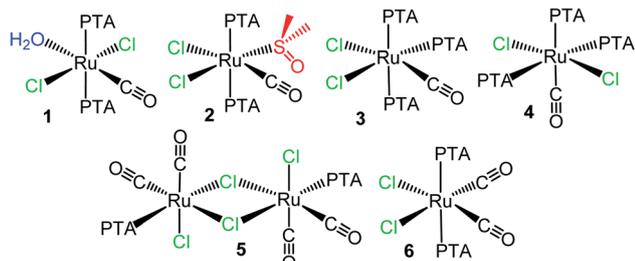
Fig. 2 Schematic structures of the neutral Ru(II)–PTA–CO precursors investigated in this paper. Top row: the monocarbonyls *trans,-trans,trans*-[RuCl₂(CO)(OH₂)(PTA)₂] (**1**), *cis,cis,trans*-[RuCl₂(CO)(dmso-S)(PTA)₂] (**2**), *cis,mer*-[RuCl₂(CO)(PTA)₃] (**3**), *trans*-[RuCl₂(CO)(PTA)₃] (**4**); bottom row: the dicarbonyls [RuCl(μ-Cl)(CO)₂(PTA)]₂ (**5**) and *cis,-cis,trans*-[RuCl₂(CO)₂(PTA)₂] (**6**). The potentially leaving ligands are colored.

report an explorative investigation on the reactivity of a series of Ru–PTA carbonyls towards the imine ligands pyridine (py) and 2,2′-bipyridine (bpy), used as models for monodentate pyridyl-linkers (*e.g.* 4,4′-bpy or pyridylporphyrins) and for chelating diimine linkers, such as 4′-methyl-2,2′-bipyridine-4-carboxylic acid (bpyAc) and 2-(2′-pyridyl)pyrimidine-4-carboxylic acid (cppH) (Fig. 1),[16] respectively.

In particular we investigated the six neutral and water-soluble Ru(II)–PTA–CO precursors shown in Fig. 2 that have at least one or two potentially labile ligands, *i.e.* H₂O, dmso-S, Cl.[15,17]

We describe here the preparation and characterization of a series of new derivatives. The compounds *trans,trans,trans*-[RuCl₂(CO)(py)(PTA)₂] (**7**), *cis,cis,trans*-[RuCl₂(CO)₂(py)(PTA)] (**9**), *cis,trans*-[Ru(bpy)Cl(CO)(PTA)₂]Cl (**10**), *mer*-[Ru(bpy)(CO)(PTA)₃][-Cl]₂ (**12**), *cis,trans*-[Ru(bpy)(CO)₂Cl(PTA)]Cl (**13**), *cis,trans*-[Ru(bpy)(CO)₂(PTA)₂](NO₃)₂ (**14NO₃**), were obtained in good yield and fully characterized, whereas *cis,cis,trans*-[RuCl₂(CO)(py)(PTA)₂] (**8**), *trans*-[RuCl₂(bpy)(CO)(PTA)] (**11**), *cis,cis*-[Ru(bpy)Cl(CO)(PTA)₂] Cl (**15**), and *cis,cis*-[Ru(bpy)(CO)₂Cl(PTA)]Cl (**16**) were either identified in solution only (**8, 15, 16**) or isolated in low amounts (**11**). The X-ray molecular structures of **7**, **11**·H₂O, and **12**·7H₂O are also reported, together with a comprehensive collection of the typical ³¹P NMR chemical shift in Ru(II)–PTA complexes as a function of the *trans* ligand.

Finally, it is interesting to note that water-soluble Ru–PTA–CO complexes and their derivatives are potentially of interest as homogeneous catalysts in aqueous medium or in biphasic systems for reactions that involve CO or CO₂,[2,8b,9,10,13,18–24] and as controlled CO-releasing and photo-releasing systems (CORMs and photoCORMs) for medicinal application.[25–35]

Results and discussion

Reactions with pyridine (py)

To the best of our knowledge, there are very few examples of Ru(II)–PTA coordination compounds with monodentate pyridine or azole ligands, *i.e.* not included in polydentate ligands.[5b,36–40] Only recently the group of Romerosa described a series of neutral Ru(II)–PTA half-sandwich compounds that
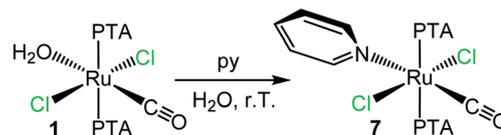
Scheme 1 Preparation of *trans,trans,trans*-[RuCl₂(CO)(py)(PTA)₂] (**7**) upon treatment of *trans,trans,trans*-[RuCl₂(CO)(OH₂)(PTA)₂] (**1**) with py in water.

bear a natural purine bound through the N7 or N9 of the imidazolic ring.[41]

When *trans,trans,trans*-[RuCl₂(CO)(OH₂)(PTA)₂] (**1**) was treated with a slight excess of pyridine in water at room temperature, the yellow complex *trans,trans,trans*-[RuCl₂(CO)(py)(PTA)₂] (**7**) was selectively obtained upon evaporation of the solvent (Scheme 1) and fully characterized by ESI-MS, NMR, and IR spectroscopies (ESI†). Thus, pyridine easily and selectively replaced the labile aqua ligand with retention of the geometry. The ³¹P{¹H} NMR spectrum of **7** (D₂O) presents a singlet at −50.0 ppm, in the typical region of mutually *trans* PTAs. The IR spectrum shows a carbonyl stretching band at 1946 cm⁻¹.

The geometry of complex **7** was confirmed by single crystal X-ray diffraction analysis (Fig. 3). In the structure, the *trans* CO/py ligands were found to be disordered by exchanging their mutual positions, with a major population of 74.7%.

Conversely, treatment of *cis,cis,trans*-[RuCl₂(CO)(dmso-S)(PTA)₂] (**2**) with a slight excess of pyridine in water afforded mixtures of products, comprising **7**, **8** (see below) and other unidentified minor species with coordinated py. However, when the reaction was performed in chloroform under microwave
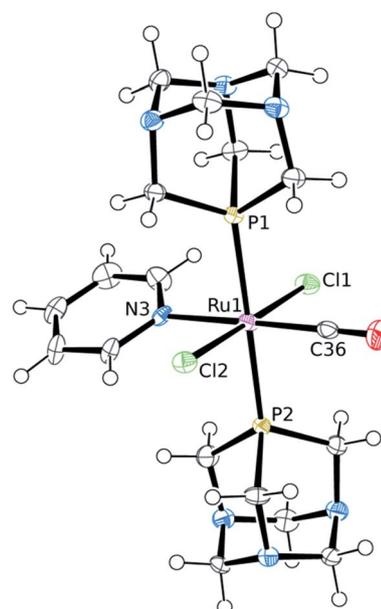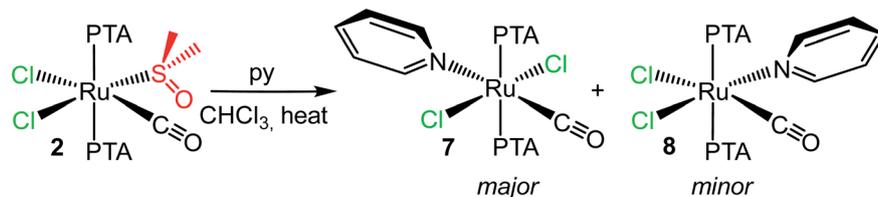

Fig. 3 X-ray molecular structure (50% probability ellipsoids) of *trans,trans,trans*-[RuCl₂(CO)(py)(PTA)₂] (**7**) (major population: 74.7%). Coordination distances (Å): Ru1–Cl1 = 2.409(1), Ru1–Cl2 = 2.419(1), Ru1–N3 = 2.207(6), Ru1–C36 = 1.861(7), Ru1–P1 = 2.349(1), Ru1–P2 = 2.344(1).

Scheme 2 Reactivity of *cis,cis,trans*-[RuCl₂(CO)(dmso-S)(PTA)₂] (**2**) with py in chloroform under MW assisted conditions (100 °C) affording a mixture of the stereoisomers *trans,trans,trans*-[RuCl₂(CO)(py)(PTA)₂] (**7**) and *cis,cis,trans*-[RuCl₂(CO)(py)(PTA)₂] (**8**).
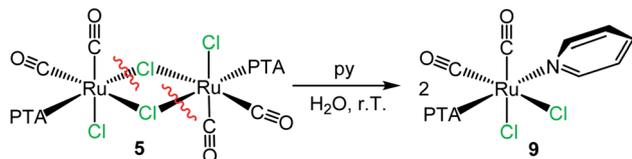
Scheme 3 Reactivity of the dinuclear species [RuCl(μ-Cl)(CO)₂(PTA)]₂ (**5**) with pyridine in water affording *cis,cis,trans*-[RuCl₂(CO)₂(py)(PTA)] (**9**).

assisted conditions (100 °C) it afforded a mixture of **7** (see above) and of a minor component (*ca.* 20%) that was identified as the stereoisomer *cis,cis,trans*-[RuCl₂(CO)(py)(PTA)₂] (**8**) (that formally derives from **2** upon replacement of the dmso without geometrical rearrangement) (Scheme 2). In fact, the main NMR resonances of **8** (*i.e.* the py signals in the proton spectrum and the singlet for the two PTAs in the phosphorous spectrum) are only slightly shifted compared to those of **7**, and integration confirmed the stoichiometry (ESI†). The IR spectrum of the mixture shows a broad carbonyl stretching band at 1977 cm⁻¹.

As previously observed by us, in aqueous solution the dinuclear species [RuCl(μ-Cl)(CO)₂(PTA)]₂ (**5**) behaves as a monomer with a formally vacant position *trans* to PTA after the selective and rapid cleavage of the chloride bridges leading to the formation of the neutral aqua species *cis,cis,trans*-[RuCl₂(CO)₂(OH₂)(PTA)].[15] Consistently, treatment of **5** with a slight excess of py in D₂O at ambient temperature afforded crystals of *cis,cis,trans*-[RuCl₂(CO)₂(py)(PTA)] (**9**). Even though the crystals were of low quality, the X-ray structure (ESI†) unambiguously confirmed the geometry of the complex, with the pyridine *trans* to PTA (first example in Ru(ɪɪ) species), *i.e.* in the place of the cleaved bridging chloride (Scheme 3).

The ESI-MS and NMR spectra of **9** in CDCl₃ (ESI;† the solubility of this species was much higher in chloroform than in water) are fully consistent with this formulation. The IR spectrum presents two bands (2058 and 1994 cm⁻¹) at frequencies

very similar to those found in the precursor **5**,[15] in agreement with the presence of two adjacent CO ligands that, in both compounds, are *trans* to chlorides. The ³¹P{¹H} NMR spectrum shows a singlet at −28.7 ppm.

Reactions with 2,2′-bipyridine (bpy)

Examples of neutral and cationic Ru(ɪɪ)–PTA complexes, containing one (*cis,cis*- and *cis,trans*-[Ru(bpy)Cl₂(PTA)₂], *fac*- and *mer*-[Ru(bpy)Cl(PTA)₃](PF₆)) or two (*cis*- and *trans*-[Ru(bpy)₂(-PTA)₂](PF₆)₂, and *cis*-[Ru(bpy)₂(OH₂)(PTA)](CF₃SO₃)₂) bpy ligands have been described by us and other groups.[7,14,42] They were obtained either by treatment of Ru–PTA precursors with bpy, or through a complementary approach (*i.e.* by reaction of Ru–bpy complexes with PTA).

In this work, we found that *trans,trans,trans*-[RuCl₂(-CO)(OH₂)(PTA)₂] (**1**) reacts with bpy in refluxing water by replacing the water molecule and one of the adjacent chlorides affording the orange cationic complex *cis,trans*-[Ru(bpy)Cl(CO)(PTA)₂]Cl (**10**) (Scheme 4).

Compound **10** was fully characterized by NMR spectroscopy and mass spectrometry. The ¹H NMR spectrum in D₂O shows eight equally intense resonances in the aromatic region, consistent with the asymmetric environment of the bpy ligand (ESI†). In agreement with previous findings,[16a,43] the highest frequency doublet was assigned to H6, *i.e.* the proton with a partial positive charge that points towards the adjacent chloride (Scheme 4). The ³¹P{¹H} NMR spectrum presents a singlet in the region of mutually *trans* PTAs (δ = −50.6 ppm). The CO stretching frequency in the IR spectrum (1984 cm⁻¹) is shifted to higher wavenumbers compared to the precursor **1** (1941 cm⁻¹), in agreement with a lower π back-bonding contribution from ruthenium because of the positive charge. With time, a very small amount of colorless crystals grew spontaneously from the D₂O NMR solution of the raw product.[44] They were found to belong to the unexpected neutral Ru(ɪɪ) complex *trans*-[RuCl₂(bpy)(CO)(PTA)] (**11**), whose formation implies replacement of one PTA. The full spectroscopic
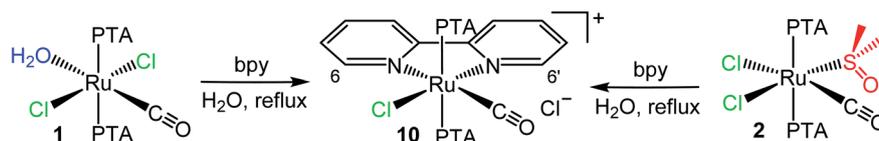
Scheme 4 Reactivity of *trans,trans,trans*-[RuCl₂(CO)(OH₂)(PTA)₂] (**1**) and *cis,cis,trans*-[RuCl₂(CO)(dmso-S)(PTA)₂] (**2**) with bpy in water affording *cis,trans*-[Ru(bpy)Cl(CO)(PTA)₂]Cl (**10**).
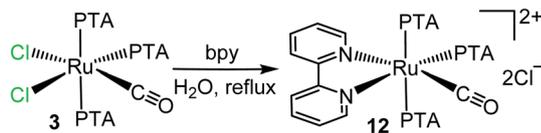
Scheme 5 Preparation of *mer*-[Ru(bpy)(CO)(PTA)$_3$](Cl)$_2$ (**12**) upon treatment of *cis,mer*-[RuCl$_2$(CO)(PTA)$_3$] (**3**) with bpy in water at reflux.
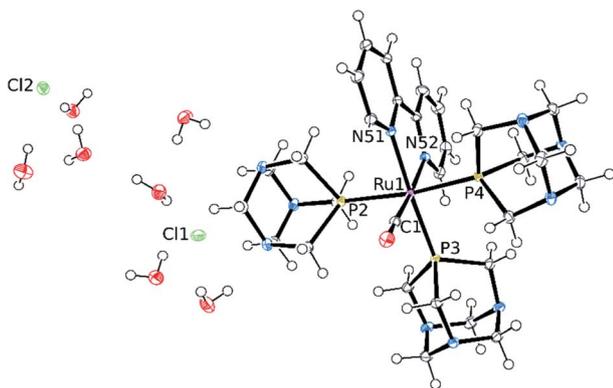

Fig. 4 X-ray molecular structure (50% probability ellipsoids) of *mer*-[Ru(bpy)(CO)(PTA)$_3$](Cl)$_2$·7H$_2$O (**12**·7H$_2$O) obtained by recrystallization of the raw product from water/acetone. Coordination distances (Å): Ru1–C1 = 1.8746(14), Ru1–N51 = 2.119(1), Ru1–N52 = 2.139(1), Ru1–P2 = 2.3650(4), Ru1–P3 = 2.3391(4), Ru1–P4 = 2.3631(4).

characterization and X-ray molecular structure of this minor species are reported in the ESI.†

Compound **10** was obtained also by treatment of *cis,cis,trans*-[RuCl$_2$(CO)(dmso-S)(PTA)$_2$] (**2**) with bpy in water (either 16 h at reflux or 30 min at 150 °C in a microwave reactor, Scheme 4). In this case bpy replaces the molecule of dmso and the adjacent chloride.

The reaction of *cis,mer*-[RuCl$_2$(CO)(PTA)$_3$] (**3**) with bpy in refluxing water led to the replacement of both chlorides by bpy, affording the orange dicationic complex *mer*-[Ru(bpy)(CO)(PTA)$_3$](Cl)$_2$ (**12**) (Scheme 5).

Compound **12** was fully characterized by NMR and IR spectroscopy, mass spectrometry, and its single-crystal X-ray structure was also determined (Fig. 4 and ESI†). The PTA region of the ^{1}H NMR spectrum in D$_2$O consists of two pairs of signals, in a 1 : 2 ratio. The two low-frequency multiplets (12H each) centered at 4.41 and 3.83 ppm and correlated in the H–H COSY spectrum, were attributed to the two equivalent *trans* PTA

ligands whose protons fall in the shielding cone of the adjacent bpy. The other two signals (6H each), centered at 4.81 ppm (partially overlapped with the water signal) and 4.65 ppm, respectively, belonged to the PTA *trans* to N. The ^{1}H–^{13}C HSQC spectrum established that, in each set, the high-frequency quartet belongs to the NC*H*$_2$N protons and the other signal to the NC*H*$_2$P protons. The downfield region of the spectrum (eight resonances, three of which overlapping in an unresolved multiplet centered at 8.42 ppm) is consistent with the asymmetric coordination environment of bpy. The aromatic protons were assigned through a 1D NOESY spectrum: saturation of the singlet of the NC*H*$_2$P protons of the PTA *trans* to bpy gave an NOE effect with the multiplet at 8.42 ppm thus implying that it contains the resonance of proton H6′, *i.e.* the one closest to the adjacent PTA. The other bpy resonances were then assigned through an H–H COSY spectrum. The ^{31}P{^{1}H} NMR spectrum presents an AX$_2$ system. The triplet that belongs to the PTA *trans* to bpy (−49.6 ppm) is upfield shifted of *ca.* 10 ppm compared to most of the known monocationic and dicationic Ru(II) complexes featuring one or two PTAs *trans* to bpy, *i.e. mer*-[Ru(bpy)Cl(PTA)$_3$](PF$_6$) (−30.2 ppm), *fac*-[Ru(bpy)Cl(PTA)$_3$](PF$_6$) (−43.5 ppm),[14] *cis*-[Ru(bpy)$_2$(PTA)$_2$](Cl)$_2$ (−38.8 ppm) and *cis*-[Ru(bpy)$_2$(PTA)(H$_2$O)](CF$_3$SO$_3$)$_2$ (−31.6 ppm).[42b] The difference might be attributed to the presence of the CO ligand in **12**.

The IR spectrum shows a carbonyl stretching band at 2010 cm^{-1}, *i.e.* at higher wavenumbers than in the precursor (1942 cm^{-1}), in agreement with the 2+ charge of **12**. For comparison, the CO stretching band in the dicationic monocarbonyl Ru(II) complex *fac*-[Ru(CO)(dmso-O)$_3$(dmso-S)$_2$](PF$_6$)$_2$ falls at 2012 cm^{-1},[45] suggesting that this parameter is not particularly affected by the nature of the ligands, but rather by the net charge of the complex.

X-ray quality crystals of **12** were obtained upon recrystallization of the raw product from water/acetone (Fig. 4). The coordination distances are in general agreement with the known *trans* influence of the ligands: thus, the Ru–P bond lengths of the two *trans* PTA ligands are longer than the Ru–P distance *trans* to N. Similarly, the Ru–N bond length *trans* to CO is longer than that *trans* to P, consistent with the previous finding that CO has a stronger *trans* influence than PTA.[14]

The reaction of *trans*-[RuCl$_2$(CO)(PTA)$_3$] (**4**) – a stereoisomer of **3** – with bpy led to a mixture of compounds (Scheme 6), identified through the ^{31}P{^{1}H} NMR spectrum as **10**, **11**, and *mer*-[Ru(bpy)Cl(PTA)$_3$]$^+$ (previously described by us as PF$_6$ salt),[14] in *ca.* 1 : 7.5 : 3 ratio. This finding suggests that, even though
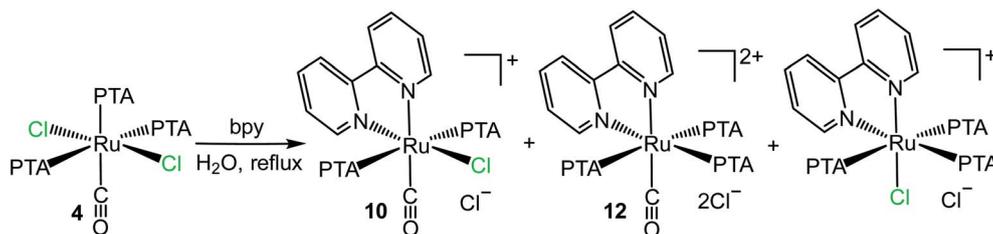
**Scheme 6** Reactivity of *trans,mer*-[RuCl$_2$(CO)(PTA)$_3$] (**4**) towards bpy in refluxing water.

Paper
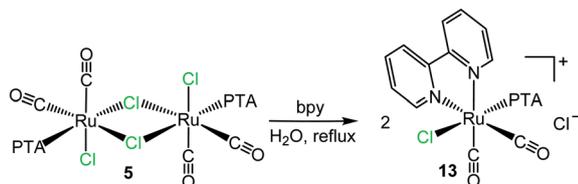
Scheme 7 Reactivity of [RuCl(μ-Cl)(CO)$_2$(PTA)]$_2$ (**5**) towards bpy in refluxing water affording *cis,trans*-[Ru(bpy)(CO)$_2$Cl(PTA)]Cl (**13**).

Scheme 9 Preparation of *cis,trans*-[Ru(bpy)(CO)$_2$(PTA)$_2$](NO$_3$)$_2$ (**14NO$_3$**).

bpy preferentially replaces the two chlorides, it can also replace either a PTA/Cl$^-$ or a CO/Cl$^-$ pair.

Treatment of the dinuclear species [RuCl(μ-Cl)(CO)$_2$(PTA)]$_2$ (**5**) with bpy in refluxing water led to the isolation of the cationic dicarbonyl red-orange compound *cis,trans*-[Ru(bpy)(CO)$_2$-Cl(PTA)]Cl (**13**), formally derived from the replacement in each half of the precursor of the two chlorides *trans* to CO, one bridging and the other terminal (Scheme 7). In fact, the ^{31}P{^{1}H} NMR spectrum in D$_2$O presents a singlet at −25.4 ppm, *i.e.* in the typical region of PTA *trans* to Cl. The ^{1}H NMR spectrum shows in the aromatic region four equally intense signals (2H each), in agreement with bpy coordinated in a symmetrical environment. The integration ratio of bpy and PTA resonances is consistent with the stoichiometry of the complex. No hydrolysis of the chloride was observed in D$_2$O solution (*i.e.* no new set of proton resonances attributable to [Ru(bpy)(CO)$_2$(OH$_2$)(-PTA)]$^{2+}$ grew with time), most likely because of the positive charge of the complex. The IR spectrum of **13** presents two CO stretching bands at 2085 and 2034 cm^{-1}, in agreement with the presence of two *cis* carbonyls. For comparison, the CO stretching bands in the cationic dicarbonyl Ru(II) complex *cis,fac*-[Ru(CO)$_2$Cl(dmso)$_3$](PF$_6$) fall at 2092 and 2030 cm^{-1}.[45]

The reaction between *cis,cis,trans*-[RuCl$_2$(CO)$_2$(PTA)$_2$] (**6**) and bpy yielded a mixture of **13** with a new product **14** (in *ca.* 1/2 ratio) (Scheme 8). The new species is characterized by a set of four equally intense bpy signals in the aromatic region of the ^{1}H NMR spectrum, and by a singlet at −50.9 ppm in the ^{31}P{^{1}H} NMR spectrum, typical of mutually *trans* PTAs. Based on this spectroscopic evidence, **14** was formulated as the dicationic complex with two mutually *trans* PTAs, *cis,trans*-[Ru(bpy)(CO)$_2$(PTA)$_2$](Cl)$_2$ (**14Cl**), derived from **6** upon replacement of both chlorides. To be noted that the formation of **13** from **6** involves isomerization: Cl, that was *trans* to CO in the precursor, is *trans* to PTA in **13**.

Compound **14** was selectively obtained, as the orange nitrate salt (**14NO$_3$**), when **6** was reacted with bpy in refluxing water after the addition of 2.1 eq. of AgNO$_3$ (Scheme 9). The ^{1}H, ^{31}P{^{1}H} NMR, and ESI-MS spectra of **14NO$_3$**, are coincident with those of **14Cl** (Scheme 8). Consistent with the *cis* geometry of
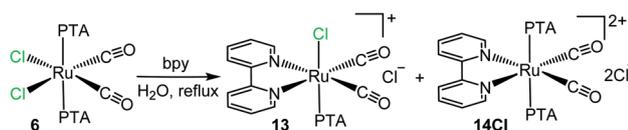
the CO ligands, the complex has two CO stretching bands (2086 and 2038 cm^{-1}) in the IR spectrum. Compared with the precursor **6**, the CO stretching frequencies of both **13** and **14** are shifted to higher wavenumbers, in accordance with the positive charge of the two products; nevertheless, it is remarkable that in **14** they are very similar to those found in **13**, despite the higher positive charge. Compound **14** is the first dicationic dicarbonyl Ru(II) compound that we have isolated thus far; the previously prepared dicationic species have a single CO (*e.g.* [Ru(CO)(dmso)$_5$](PF$_6$)$_2$), whereas the dicarbonyl compounds were monocationic (*e.g.* **13**).

Light-induced rearrangements in Ru(II)–PTA–bpy carbonyls

Both Ru(II)–PTA and RuX$_2$(CO)$_n$(P)$_{4−n}$ ($n = 1–3$) complexes have shown to be photoreactive.[14,15,24,46–49] The group of Romerosa has recently reported a study of the effects of visible light on a series of water-soluble Ru(II) complexes with PTA.[24] For this reason we decided to perform a preliminary investigation of the effect of visible light on selected Ru(II)–PTA–bpy carbonyls, that are characterized by the presence of an absorption band in the range of 400–525 nm. In general, D$_2$O solutions of the complexes were directly irradiated in the NMR tube and the products were characterized spectroscopically, without being isolated.

We found that 24 h irradiation with blue light ($\lambda = 470$ nm) of an orange D$_2$O solution of *cis,trans*-[Ru(bpy)Cl(CO)(PTA)$_2$]Cl (**10**) induces its clean and complete transformation to the new *cis*-isomer *cis,cis*-[Ru(bpy)Cl(CO)(PTA)$_2$]Cl (**15**) (Scheme 10). In fact, the ^{31}P{^{1}H} NMR spectrum of the product (ESI†) presents an AX system of two doublets, one in the region of PTA *trans* to Cl (−25.1 ppm, $^2J_{P–P} = 24.7$ Hz) and the second in that of PTA *trans* to bpy (−42.3 ppm). The PTA region of the ^{1}H NMR spectrum shows a broad singlet at 3.93 ppm and three partially overlapped AB systems centered respectively at 4.41, 4.58, and 4.71 ppm (4H each), consistent with the non-equivalence of the two PTAs. The two most upfield signals, correlated in the ^{1}H–^{1}H COSY spectrum (ESI†), were attributed to the PTA *trans* to Cl that falls into the shielding cone of the adjacent bpy. As above

Scheme 8 Reactivity of *cis,cis,trans*-[RuCl$_2$(CO)$_2$(PTA)$_2$] (**6**) towards bpy in refluxing water yielding a mixture of *cis,trans*-[Ru(bpy)(CO)$_2$-Cl(PTA)]Cl (**13**) and *cis,trans*-[Ru(bpy)(CO)$_2$(PTA)$_2$](Cl)$_2$ (**14Cl**).
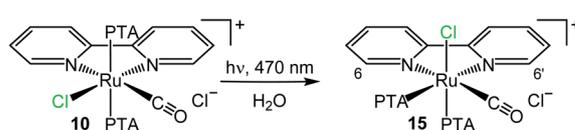
Scheme 10 Light-induced isomerization ($\lambda = 470$ nm, 24 h) of *cis,trans*-[Ru(bpy)Cl(CO)(PTA)$_2$]Cl (**10**) to *cis,cis*-[Ru(bpy)Cl(CO)(PTA)$_2$]Cl (**15**).
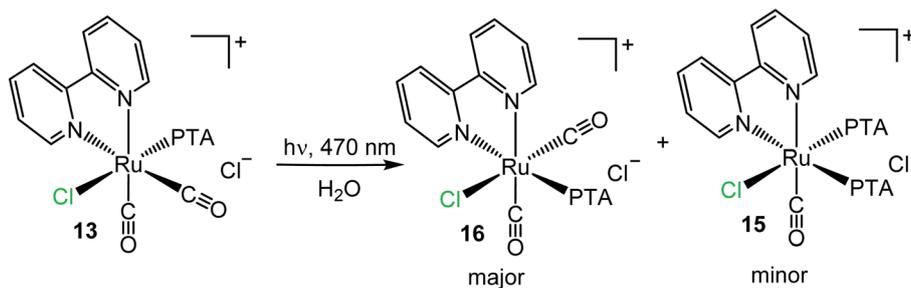
Scheme 11 Light-induced isomerization ($\lambda = 470$ nm, 72 h) of *cis,trans*-[Ru(bpy)(CO)$_2$Cl(PTA)]Cl (**13**) to *cis,cis*-[Ru(bpy)(CO)$_2$Cl(PTA)]Cl (**16**) and *cis,cis*-[Ru(bpy)Cl(CO)(PTA)$_2$]Cl (**15**).

Table 1 The main Ru(II)–PTA–pyridine carbonyls described in this work
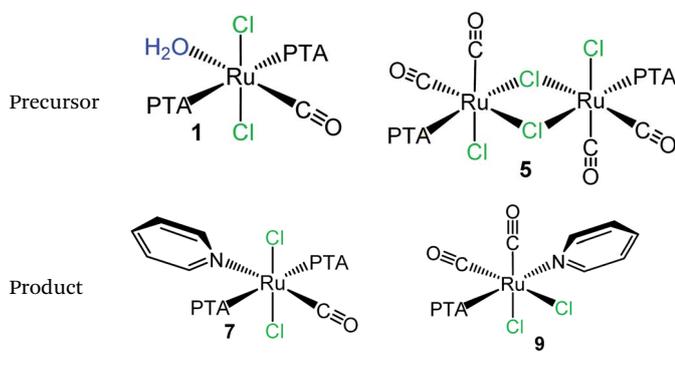
for **12**, the aromatic protons were assigned through a 1D NOESY spectrum, followed by an ^{1}H–^{1}H COSY spectrum (ESI†). Finally, the IR spectrum of compound **15** shows a single carbonyl stretching band at 1992 cm^{-1}, *i.e.* a frequency similar to that of the *trans*-isomer **10** (1984 cm^{-1}).

A similar light-induced isomerization was observed with *cis,trans*-[Ru(bpy)(CO)$_2$Cl(PTA)]Cl (**13**) (Scheme 11). In this case the process was slower (and less selective) and complete

transformation required the irradiation of an aqueous solution of **13** with blue light for 3 days. The major product of this reaction, **16**, shows a singlet in the region of PTA *trans* to bpy (-39.6 ppm) in the ^{31}P{^{1}H} NMR spectrum, and eight resonances in the aromatic region of the ^{1}H NMR spectrum for an asymmetrically bound bpy (with two multiplets of overlapping resonances). Consistent with these spectroscopic evidence, the new compound **16** was formulated as *cis,cis*-[Ru(bpy)(CO)$_2$-Cl(PTA)]Cl. The IR spectrum presents two carbonyl stretching bands at 2006 and 1979 cm^{-1} in agreement with the presence of two *cis* CO ligands. Compared to the starting *trans* isomer **13** (2085 and 2034 cm^{-1}), the two bands of **16** are shifted to lower wavenumbers, possibly because one CO is *trans* to the good π-donor Cl.

To our surprise, the ^{31}P{^{1}H} NMR spectrum showed that formation of **16** is accompanied by that of **15** (*ca.* 6/1 ratio), in addition to other uncharacterized minor species (ESI†). Since there is no external source of PTA, the formation of **15** from **13** implies the occurrence of a decarbonylation process followed by disproportionation.

Conversely, compound *cis,trans*-[Ru(bpy)(CO)$_2$(PTA)$_2$](NO$_3$)$_2$ (**14NO$_3$**) was light-stable. The ^{31}P NMR spectrum of a D$_2$O solution of **14NO$_3$** remained unchanged even after one week of irradiation either with blue or white light.

Table 2 The main Ru(II)–PTA–bpy carbonyls described in this work listed in order of increasing number of PTA ligands
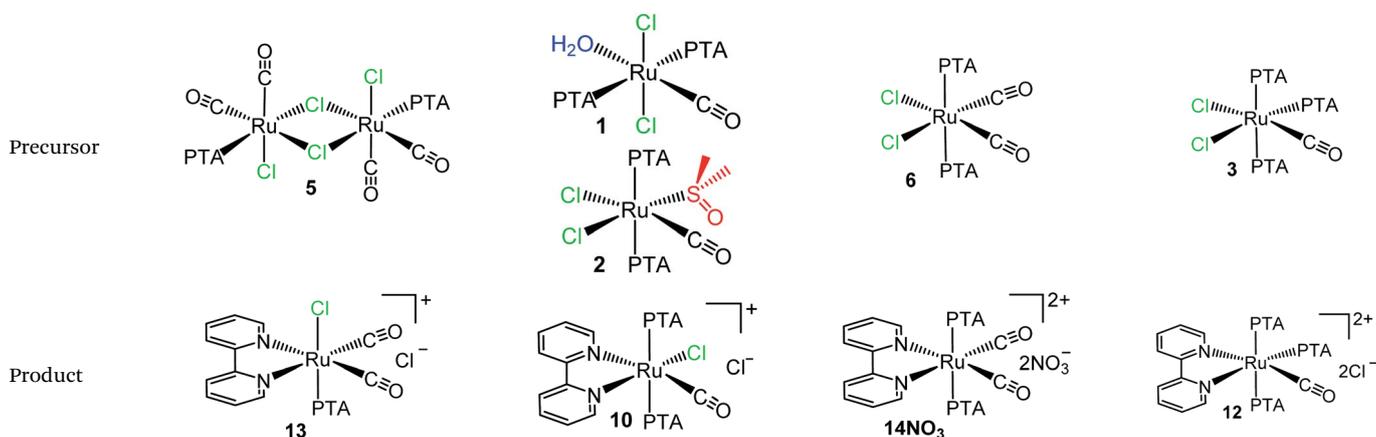
Table 3 Typical $^{31}P\{^1H\}$ NMR chemical shift intervals (Δ) and Ru–P distances for PTA bound to octahedral Ru(II) complexes as a function of the nature of the *trans* ligand

Ligand *trans* to PTA	Δ $^{31}P\{^1H\}^a$ (ppm)	Δ Ru–P distance (Å)	Ref.^{b}
OH$_2$/OH	−5 ÷ −16	—	14, 15, 24 and 50
Cl	−14 ÷ −30	2.232 ÷ 2.283	p.w. and 8b, 14 and 15
N(azole)	−17 ÷ −49	2.2605 ÷ 2.2971	36–40
Br	−24 ÷ −27	2.266 ÷ 2.281	51
H	−26.6^c	2.299 ÷ 2.300	48
N(py)^c	−28.8		p.w.
S^d	−30 ÷ −45	2.280 ÷ 2.318	12, 16b and 43
N(bpy, phen)	−30 ÷ −50^e	2.2849 ÷ 2.3391^f	p.w. and 7, 14 and 42b
P(PTA)	−42 ÷ −60	2.290 ÷ 2.400	p.w. and, 7, 8b, 13–15, 24, 42, 48, 50 and 52–54
CO	−55 ÷ −70	2.3821 ÷ 2.3828	15
C^g	−68.4	2.395(1)	55

^{a} For comparison, the singlet of free PTA falls at δ = −98.2 ppm in D$_2$O and at −102.3 ppm in CDCl$_3$. ^{b} p.w. = present work. ^{c} Single hit. ^{d} From [9] aneS3 = 1,4,7-trithiacyclononane. ^{e} When PTA is trans to 2,2′-bipyridine-6,6′-dicarboxylato (bda), the $^{31}P\{^1H\}$ chemical shift falls at −51.2 ppm (not included in the table).^{54} ^{f} Concerns bpy complexes exclusively. In the single phen complex, *mer*-[Ru(phen)Cl(PTA)$_3$]Cl (two independent cations in the asymmetric unit), the Ru–P distances are slightly shorter, 2.269(3) and 2.279(3) Å.^{42b} ^{g} Single hit, from cyclometallated 2-phenylpyridine.

Conclusions

We have investigated the reactivity of selected neutral Ru(II)–PTA carbonyls with potentially labile ligands (*i.e.* H$_2$O, dmso and/or Cl) towards the model imine ligands pyridine (py) and 2,2′-bipyridine (bpy). The results are graphically summarized in Tables 1 and 2 that collect the main products with their respective precursors. To be noted that **5** is the only precursor that affords derivatives with a single PTA bound to ruthenium. Whereas the monodentate pyridine replaces exclusively neutral ligands, *i.e.* H$_2$O or dmso-S, bpy is capable of replacing also the chlorides, thus affording mono- and dicationic products. PTA and supporting CO ligands are typically not replaced. Consistent with the expected lability order, the aqua ligand is easily replaced by pyridine at room temperature (*e.g.* **7**), whereas replacement of dmso-S required more forcing conditions (refluxing chloroform or ethanol) that induced partial isomerization. Replacement of chlorides by bpy was typically performed in refluxing water, and was occasionally silver-assisted. Most of the complexes are well soluble in water and alcohols (methanol and ethanol). Exceptions are the neutral carbonyls **9** and **11**, both containing a single PTA ligand.

Coordination of bpy is often accompanied by stereochemical changes. We notice that bpy does not like being bound *trans* to two PTA ligands. In fact, in all the Ru(II)–PTA–bpy complexes described in the literature that feature two or three PTA ligands, the coplanar {Ru(bpy)(PTA)$_2$} fragment is found only in *fac*-[Ru(bpy)Cl(PTA)$_3$](PF$_6$), that however is a kinetic product that thermally isomerizes to the thermodynamic meridional stereoisomer.[14] We believe that this is due to both steric and electronic factors (π back-bonding competition).

We found that in some bpy compounds light-induced isomerization could be induced. Thus, irradiation with blue light selectively transformed *cis*,*trans*-[Ru(bpy)Cl(CO)(PTA)$_2$]Cl (**10**) into *cis*,*cis*-[Ru(bpy)Cl(CO)(PTA)$_2$]Cl (**15**) (Scheme 10), whereas the isomerization of *cis*,*trans*-[Ru(bpy)(CO)$_2$Cl(PTA)]Cl

(**13**) to *cis*,*cis*-[Ru(bpy)(CO)$_2$Cl(PTA)]Cl (**16**) was accompanied by formation of **15** (Scheme 11).

We have already observed that is possible to use $^{31}P\{^1H\}$ NMR chemical shifts as a diagnostic tool for establishing the geometry of octahedral Ru–PTA complexes.[14,15] We report here an updated list of the typical $^{31}P\{^1H\}$ NMR chemical shift intervals (Δ) for PTA bound to Ru(II) as a function of the nature of the *trans* ligand, that contains the data from the new py and bpy derivatives (Table 3). We observe that when PTA is *trans* to an imine nitrogen (*i.e.* py, bpy), the $^{31}P\{^1H\}$ NMR chemical shift is remarkably affected by the nature of the ligand: when *trans* to py it falls at −28 ppm (we have only one example: complex **9**), whereas when *trans* to bpy it falls in a rather broad range which is shifted to lower frequencies compared to py: −30 ÷ −50 ppm (but most often between −30 a −40 ppm, see below). Pyridine is known to be a weaker field ligand compared to bpy, being both a worse σ-donor and π-acceptor. In addition, the orientation of the pyridyl rings are different: for bpy they are in the plane containing PTA, whereas pyridine is typically canted with respect to such plane, implying a different involvement of their π orbitals. Indeed, in the complex *trans*-[RuCl$_2${(R,R)-^{i}Pr-pybox}(PTA)] where pyridine is part of a tridentate chelating ligand, and is forced to lay in the equatorial plane that contains the *trans* PTA, the ^{31}P chemical shift falls at −41.5 ppm, *i.e.* in the range typical for bpy.[5b]

As already observed by us,[14,15] Table 3 provides also a *trans*-influence ranking for the ligands *trans* to PTA; in fact there is a rough correlation between the Ru–P bond length and the chemical shift of the $^{31}P\{^1H\}$ NMR resonance: as the Ru–P distance increases, the phosphorous resonance shifts progressively to lower frequencies (*i.e.* closer to that of free PTA). To this regard we notice that there are only two examples of PTA *trans* to bpy in which the ^{31}P chemical shift falls at frequencies lower than −40 ppm: *fac*-[Ru(bpy)Cl(PTA)$_3$](PF$_6$) (−43.5 ppm) and *mer*-[Ru(bpy)(CO)(PTA)$_3$](Cl)$_2$ (**12**, −49.6 ppm). In both complexes, due to the overall charge and competing ligands, the π-back

donation to such PTAs is expected to be lower than for the other cases, leading to weaker and longer Ru–P bonds.

Experimental section

Materials

All chemicals were purchased from Sigma-Aldrich and used as received. Solvents were of reagent grade. The Ru(II)–PTA carbonyls **1–6** were synthesized and purified as previously reported by us.[15]

Instrumental methods

Mono- and bi-dimensional (^{1}H–^{1}H COSY, ^{1}H–^{13}C HSQC) NMR spectra were recorded at room temperature on a Varian 400 or 500 spectrometer (^{1}H: 400 or 500 MHz, ^{13}C{^{1}H}: 100.5 or 125.7 MHz, ^{31}P{^{1}H}: 161 or 202 MHz). ^{1}H and ^{13}C{^{1}H} chemical shifts were referenced to the peak of residual non-deuterated solvent ($\delta = 7.26$ and 77.16 for CDCl$_3$, 2.50 and 39.52 for DMSO-d_6) or were measured relative to the internal standard DSS ($\delta = 0.00$) for D$_2$O. Carbon resonances were assigned through the HSQC spectra. ^{31}P chemical shifts were referenced to external 85% H$_3$PO$_4$ at 0.00 ppm. ESI mass spectra were collected in the positive and negative mode on a PerkinElmer APII spectrometer at 5600 eV. The UV-vis spectra were obtained on an Agilent Cary 60 spectrophotometer, using 1.0 cm path-length quartz cuvettes (3.0 mL). Solid state infrared spectra were obtained as Nujol mulls between NaCl plates and recorded on a PerkinElmer Fourier-transform IR/Raman 2000 instrument in the transmission mode. Solution IR spectra (in chloroform, ethanol or methanol) in the CO stretching region were recorded between CaF$_2$ windows (0.5 mm spacer). A thermostatted Berghof stainless steel vessel (autoclave), equipped with a 100 mL Teflon liner, was used for the reactions with CO under pressure. A CEM Discover microwave reactor was used for the microwave-assisted reactions performed in 10 mL vessels. Elemental analyses were performed in the Department of Chemistry of the University of Bologna (Italy). A homemade LED apparatus, described in detail elsewhere,[56] was used for performing the photochemical reactions in NMR tubes.

X-ray diffraction

Data collections were performed at the X-ray diffraction beamline (XRD1) of the Elettra Synchrotron of Trieste (Italy) equipped with a Pilatus 2 M image plate detector.

Collection temperature was 100 K (nitrogen stream supplied through an Oxford Cryostream 700); the wavelength of the monochromatic X-ray beam was 0.700 Å and the diffractograms were obtained with the rotating crystal method. The crystals were dipped in N-paratone and mounted on the goniometer head with a nylon loop. The diffraction data were indexed, integrated and scaled using the XDS code.[57] The structures were solved by the dual space algorithm implemented in the SHELXT code.[58] Fourier analysis and refinement were performed by the full-matrix least-squares methods based on F2 implemented in SHELXL.[59] The Coot program was used for modeling.[60] Anisotropic thermal motion was allowed for all non-hydrogen atoms.

Hydrogen atoms were placed at calculated positions with isotropic factors $U = 1.2 \times U_{eq.}$, $U_{eq.}$ being the equivalent isotropic thermal factor of the bonded non hydrogen atom. Crystal data and details of refinements are in the ESI.†

Synthesis of the complexes

All the synthetic procedures with Ru–PTA carbonyls precursors were performed under dimmed light and in light-protected glassware.

***trans,trans,trans*-[RuCl$_2$(CO)(py)(PTA)$_2$]** **(7).** *trans,trans,trans*-[RuCl$_2$(CO)(OH$_2$)(PTA)$_2$]·3H$_2$O (**1**, 30 mg, 0.051 mmol) was dissolved in 3 mL of water obtaining a yellow solution; 1.4 equivalents of pyridine (13.1 μL, 0.07 mmol) were added and the solution was stirred at room temperature for three days. Removal of the water by rotary evaporation afforded a yellow precipitate that was treated with acetone (2 × 2 mL). The resulting yellow powder was collected on a glass filter, washed with acetone and diethyl ether, and dried *in vacuo* (yield: 19.2 mg, 63%). The solid was pure **7** according to ^{1}H and ^{31}P{^{1}H} NMR spectra. Elemental analysis calcd for [C$_{18}$H$_{29}$Cl$_2$-N$_7$OP$_2$Ru] (M_W: 593.0): C 36.43; H 4.93; N 16.52. Found: C 36.53; H 4.89; N 16.59. ^{1}H NMR (D$_2$O) δ (ppm): 9.08 (d, 2H, H2, 6), 8.11 (t, 1H, H4), 7.66 (t, 2H, H3, 5), 4.35 (m, 12H, NC*H*$_2$N), 3.90 (br s, 12H, NC*H*$_2$P). ^{13}C NMR from the HSQC spectrum (D$_2$O), δ (ppm): 151.0 (C2, 6), 139.6 (C4), 125.9 (C3, 5), 70.6 (N*C*H$_2$N), 47.0 (N*C*H$_2$P). ^{31}P{^{1}H} NMR (D$_2$O), δ (ppm): −50.0 (s, 2P, mutually *trans* PTAs). Selected IR absorption (Nujol, cm^{-1}): 1946 (ν_{CO}). ESI mass spectrum: 594.3 m/z [M + H]$^+$ (calcd 594.0).

***cis,cis,trans*-[RuCl$_2$(CO)$_2$(py)(PTA)]** **(9).** [RuCl(μ-Cl)(CO)$_2$(-PTA)]$_2$ (**5**, 30 mg, 0.038 mmol) was partially dissolved in 3 mL of water obtaining a colorless solution; 1.2 equivalents of pyridine (16.0 μL, 0.091 mmol) were added and the solution was stirred at room temperature for three days. Removal of the water by rotary evaporation afforded a precipitate that was dissolved in chloroform (a small amount of undissolved solid was removed by filtration over Celite). Removal of the chloroform by rotary evaporation afforded a solid that was pure **9** according to ^{1}H and ^{31}P{^{1}H} NMR spectra (yield: 7.3 mg, 55%). X-ray quality crystals of **9** formed spontaneously from a concentrated D$_2$O solution. Elemental analysis calcd for [C$_{13}$H$_{17}$Cl$_2$N$_4$O$_2$PRu] (M_W: 463.9): C 32.63; H 3.69; N 12.07. Found: C 32.54; H 3.59; N 11.95. ^{1}H NMR (CDCl$_3$) δ (ppm): 8.91 (d, 2H, H2, 6), 7.87 (t, 1H, H4), 7.45 (t, 2H, H3, 5), 4.60 (br s, 6H, NC*H*$_2$N), 4.53 (br s, 6H, NC*H*$_2$P). ^{13}C NMR from the HSQC spectrum (CDCl$_3$), δ (ppm): 154.2 (C2, 6), 138.8 (C4), 125.8 (C3, 5), 73.1 (N*C*H$_2$N), 53.5 (N*C*H$_2$P). ^{31}P{^{1}H} NMR (CDCl$_3$), δ (ppm): −28.8 (s, 1P, PTA *trans* to py). Selected IR absorption (chloroform solution, cm^{-1}): 2058 (ν_{CO}), 1994 (ν_{CO}). ESI mass spectrum: 464.5 m/z [M + H]$^+$ (calcd 464.9).

***cis,trans*-[Ru(bpy)Cl(CO)(PTA)$_2$]Cl** **(10).** *cis,cis,trans*-[RuCl$_2$(-CO)(OH$_2$)(PTA)$_2$]·3H$_2$O (**1**, 20 mg, 0.034 mmol) was dissolved in 5 mL of water. One eq. of bpy (5.3 mg, 0.034 mmol) was added and the mixture was refluxed for 2 h. The yellow solution turned rapidly orange. The solvent was removed by rotary evaporation affording an orange solid. The solid was pure **10**, according to ^{1}H and ^{31}P{^{1}H} NMR spectra (yield 22.3 mg, 98%). Elemental analysis calcd for [C$_{23}$H$_{32}$Cl$_2$N$_8$OP$_2$Ru] (M_W: 670.5): C 41.20; H

4.81; N 16.71. Found: C 41.12; H 4.86; N 16.77. ^{1}H-NMR (D$_2$O) δ (ppm): 9.27 (d, 1H, H6), 8.93 (d, 1H, H6′), 8.66 (d, 1H, H3), 8.55 (d, 1H, H3′), 8.42 (t, 1H, H4), 8.23 (t, 1H, H4′), 7.96 (t, 1H, H5), 7.60 (d, 1H, H5′), 4.41, 4.31 (ABq, 12H, NCH$_2$N), 3.82, 3.76 (ABq, 12H, NCH$_2$P). ^{13}C NMR from the HSQC spectrum (D$_2$O), δ (ppm): 155.7 (C6′), 149.0 (C6), 141.0 (C4), 139.4 (C4′), 128.1 (C5′), 127.9 (C5), 125.0 (C3′), 124.8 (C3), 70.3 (NCH$_2$N), 46.3 (NCH$_2$P). ^{31}P{^{1}H} NMR (D$_2$O), δ (ppm): −50.6 (s, 2P, mutually *trans* PTAs). Selected IR absorption (ethanol solution, cm^{-1}): 1984 (ν_{CO}). ESI mass spectrum: 635.6 *m/z* [M$^+$] (calcd 635.9). UV-vis (H$_2$O): λ_{max} = 401 nm.

Compound **10** was also obtained, in lower yield, by treatment of an aqueous solution of *cis,cis,trans*-[RuCl$_2$CO(dmso-S)(PTA)$_2$] (**2**) (40.0 mg, 0.067 mmol) with bpy (10.5 mg, 0.067 mmol) for 16 h at reflux or in a microwave reactor at 150 °C for 30 min. The solvent was removed by rotary evaporation affording an orange solid that was crushed with acetone (2 × 2 mL), then washed with diethyl ether, and dried *in vacuo* (yield 25.6 mg, 57%).

mer-[**Ru(bpy)(CO)(PTA)$_3$](Cl)$_2$ (12).** *cis,mer*-[RuCl$_2$CO(PTA)$_3$] (**3**) (40.0 mg, 0.060 mmol) was dissolved in 5 mL of water. One eq. of bpy (9.4 mg, 0.060 mmol) was added and the yellow solution was refluxed for 1 h, during which time it turned rapidly to orange (10 min). The solvent was removed by rotary evaporation affording an orange solid that was treated with acetone (2 × 2 mL), washed with diethyl ether and dried *in vacuo*. The solid was pure **12**, according to ^{1}H and ^{31}P{^{1}H} NMR spectra (yield 30.0 mg, 60%). X-ray quality crystals of **12** were obtained by slow diffusion of acetone into a water solution of the complex. Complex **12** is soluble in water, methanol, ethanol and DMSO. Elemental analysis calcd for [C$_{29}$H$_{44}$Cl$_2$N$_{11}$OP$_3$Ru] (M_W: 826.6): C 42.09; H 5.36; N 18.62. Found: C 42.00; H 5.25; N 18.54. ^{1}H-NMR (D$_2$O) δ (ppm): 9.07 (d, 1H, H6), 8.92 (m, 2H, H3 + H3′), 8.53 (m, 3H, H6′ + H4 + H4′), 7.99 (m, 2H, H5 + H5′), 4.85, 4.73 (ABq, 6H, NCH$_2$N PTA *trans* to N), 4.66 (br s, 6H, NCH$_2$P, PTA *trans* to N) 4.40 (m, 12H, NCH$_2$N mutually *trans* PTAs), 3.86, 3.80 (ABq, 12H, NCH$_2$P). ^{13}C NMR from the HSQC spectrum (D$_2$O), δ (ppm): 154.9 (C6), 153.8 (C6′), 142.4 (C4 + C4′), 129.9 (C5 + C5′), 126.9 (C3 + C3′). ^{31}P{^{1}H} NMR (D$_2$O), δ (ppm): −49.6 (t, 1P, $^2J_{P-P}$ = 25.2 Hz, PTA *trans* to N), −55.4 (d, 2P, mutually *trans* PTAs). Selected IR absorption (Nujol, cm^{-1}): 2010 (ν_{CO}). ESI mass spectrum: 631.6 *m/z* [M − PTA + OH]$^+$ (calcd 631.7). UV-vis (H$_2$O): λ_{max} = 415 nm.

cis,trans-[**Ru(bpy)(CO)$_2$Cl(PTA)]Cl (13).** [RuCl(μ-Cl)(CO)$_2$(PTA)]$_2$ (**5**, 30 mg, 0.038 mmol) was dissolved in 5 mL of water. One eq. of bpy (5.9 mg, 0.038 mmol) was added and the colorless solution was refluxed for 1 h, during which time it turned rapidly to orange-red. The solvent was removed by rotary evaporation affording an orange solid that was treated with acetone (2 × 2 mL), washed with diethyl ether, and dried *in vacuo*. The solid was pure **13**, according to ^{1}H and ^{31}P{^{1}H} NMR spectra (yield 13.4 mg, 65%). Elemental analysis calcd for [C$_{18}$H$_{20}$Cl$_2$-N$_5$O$_2$PRu] (M_W: 541.3): C 39.94; H 3.72; N 12.94. Found: C 39.84; H 3.66; N 12.85. ^{1}H-NMR (D$_2$O) δ (ppm): 9.08 (d, 2H, H6, 6′), 8.67 (d, 2H, H3, 3′) 8.44 (t, 2H, H4, 4′), 7.91 (t, 2H, H5, 5′), 4.46 (m, 6H, NCH$_2$N), 4.09 (br s, 6H, NCH$_2$P). ^{13}C NMR from the HSQC spectrum (D$_2$O), δ (ppm): 153.5 (C6, 6′), 142.0 (C4, 4′), 129.0 (C5, 5′), 125.5 (C3, 3′), 70.3 (NCH$_2$N), 50.6 (NCH$_2$P). ^{31}P{^{1}H} NMR

(D$_2$O), δ (ppm): −25.5 (s, 1P, PTA *trans* to Cl). Selected IR absorption (methanol solution, cm^{-1}): 2085 (ν_{CO}), 2034 (ν_{CO}). ESI mass spectrum: 478.6 *m/z* [M − CO]$^+$ (calcd 478.7). UV-vis (H$_2$O): λ_{max} = 526 nm.

cis,trans-[**Ru(bpy)(CO)$_2$(PTA)$_2$](NO$_3$)$_2$ (14NO$_3$).** *cis,cis,trans*-[RuCl$_2$CO$_2$(PTA)$_2$] (**7**) (40.0 mg, 0.074 mmol) was dissolved in 8 mL of water. 2.1 eq. of AgNO$_3$ (26.4 mg, 0.155 mmol) and 1 eq. of bpy (11.6 mg, 0.074 mmol) were added and the mixture was heated to reflux for 1 h. Upon heating the colorless solution turned rapidly orange-red, and a grey AgCl precipitate formed. At the end of reaction, the precipitate was removed by filtration on a Celite pad. The solution was rotary evaporated to dryness affording a red solid that was treated with acetone (3 × 2 mL), washed with diethyl ether, and dried *in vacuo*. The solid was pure **14NO$_3$**, according to ^{1}H and ^{31}P{^{1}H} NMR spectra (yield 30.0 mg, 57%). Complex **14NO$_3$** well soluble in water and DMSO. Elemental analysis calcd for [C$_{24}$H$_{32}$N$_{10}$O$_8$P$_2$Ru] (M_W: 751.6): C 38.35; H 4.29; N 18.64. Found: C 38.20; H 4.22; N 18.73. ^{1}H-NMR (D$_2$O), δ (ppm): 9.02 (d, 2H, H6, 6′), 8.82 (d, 2H, H3, 3′) 8.57 (t, 2H, H4, 4′), 8.02 (t, 2H, H5, 5′), 4.47, 4.43 (ABq, 12H, NCH$_2$N), 4.04 (br s, 12H, NCH$_2$P). ^{13}C NMR from the HSQC spectrum (D$_2$O), δ (ppm): 153.9 (C6, 6′), 142.7 (C4, 4′), 129.1 (C5, 5′), 126.7 (C3, 3′), 70.4 (NCH$_2$N), 47.8 (NCH$_2$P). ^{31}P{^{1}H} NMR (D$_2$O), δ (ppm): −50.9 (s, 2P, mutually *trans* PTAs). Selected IR absorption (methanol solution, cm^{-1}): 2086 (ν_{CO}), 2038 (ν_{CO}). UV-vis (H$_2$O): λ_{max} = 523 nm.

cis,cis-[**Ru(bpy)Cl(CO)(PTA)$_2$]Cl (15).** The reaction was performed in an NMR tube, and the product was not isolated. *cis,trans*-[Ru(bpy)Cl(CO)(PTA)$_2$]Cl (**23**, 5.0 mg, 7 μmol) was dissolved in 0.6 mL of D$_2$O, and the orange solution was irradiated with blue light (λ = 470 nm, 40 mW) for 24 h. Even though no evident color change was observed during the reaction, the final ^{1}H and ^{31}P{^{1}H} NMR spectra indicated complete formation of **15**. ^{1}H-NMR (D$_2$O) δ (ppm): 9.09 (d, 1H, H6), 8.75 (d, 1H, H6′), 8.65 (d, 1H, H3), 8.58 (d, 1H, H3′), 8.41 (t, 1H, H4), 8.32 (t, 1H, H4′), 7.87 (t, 1H, H5), 7.81 (d, 1H, H5′), 4.61 (m, 6H, NCH$_2$N), 4.45 (m, 6H NCH$_2$P) 4.31, 4.16 (ABq, 6H, NCH$_2$N), 3.80 (br s, 12H, NCH$_2$P). ^{13}C NMR from the HSQC spectrum (D$_2$O), δ (ppm): 153.4 (C6), 153.3 (C6′), 141.5 (C4), 140.7 (C4′), 128.4 (C5), 128.1 (C5′), 125.5 (C3), 125.0 (C3), 70.6 (NCH$_2$N), 70.3 (NCH$_2$N), 80.8 (NCH$_2$P), 49.0 (NCH$_2$P). ^{31}P NMR (D$_2$O), δ (ppm): −25.0 (1P, $^2J_{P-P}$ = 24.8 Hz, PTA *trans* to Cl), −42.4 (1P, PTA *trans* to N). Selected IR absorption (cm^{-1}): 1992 (ν_{CO}). ESI mass spectrum: 635.4 *m/z* (635.9 calcd) (M$^+$). UV-vis (H$_2$O): λ_{max} = 405 nm.

cis,cis-[**Ru(bpy)(CO)$_2$Cl(PTA)]Cl (16).** The reaction was performed in an NMR tube, and the product was not isolated. *cis,trans*-[Ru(bpy)(CO)$_2$Cl(PTA)]Cl (**13**, 2.5 mg, 4 μmol) was dissolved in 0.6 mL of D$_2$O, and the orange-red solution was irradiated with blue light (λ = 470 nm, 40 mW) for 72 h. The solution turned from orange-red to orange during the reaction. The final ^{1}H and ^{31}P{^{1}H} NMR spectra indicated complete formation of **16** in mixture with *cis,cis*-[Ru(bpy)Cl(CO)(PTA)$_2$]Cl (**15**) (6/1 ratio *ca.*). ^{1}H-NMR (D$_2$O) δ (ppm): 9.28 (d, 1H, H6), 8.77 (d, 1H, H6′), 8.61 (d, 1H, H3), 8.44 (m, 3H, H3′ + H4 + H4′), 7.92 (m, 2H, H5 + H5′), 4.47 (m, 6H, NCH$_2$N), 4.05, 4.01 (ABq, 6H NCH$_2$P). ^{13}C NMR from the HSQC spectrum (D$_2$O), δ (ppm):

155.8 (C6), 155.5 (C6′), 140.7 (C4 + C4′), 128.3 (C5 + C5′), 125.8 (C3′), 125.5 (C3), 70.5 (NCH_2N), 48.4 (NCH_2P). $^{31}P\{^1H\}$ NMR (D$_2$O), δ (ppm): −39.6 (s, 1P, PTA *trans* to N). Selected IR absorption (ethanol solution, cm^{-1}): 2006 (ν_{CO}), 1979 (ν_{CO}). ESI mass spectrum: 478.6 *m/z* [M − CO]$^+$ (calcd 478.7). UV-vis (H$_2$O): λ_{max} = 400 nm.

Conflicts of interest

There are no conflicts to declare.

Acknowledgements

References

1 (*a*) D. J. Daigle, A. B. Pepperman Jr and S. L. Vail, *J. Heterocycl. Chem.*, 1974, **11**, 407–408; (*b*) D. J. Daigle, T. J. Decuir, J. B. Robertson and D. J. Darensbourg, *Inorg. Synth.*, 1998, **32**, 40–45.

2 (*a*) A. D. Phillips, L. Gonsalvi, A. Romerosa, F. Vizza and M. Peruzzini, *Coord. Chem. Rev.*, 2004, **248**, 955–993; (*b*) J. Bravo, S. Bolaño, L. Gonsalvi and M. Peruzzini, *Coord. Chem. Rev.*, 2010, **254**, 555–607; (*c*) A. Guerriero, M. Peruzzini and L. Gonsalvi, *Coord. Chem. Rev.*, 2018, **355**, 328–361.

3 D. N. Akbayeva, L. Gonsalvi, W. Oberhauser, M. Peruzzini, F. Vizza, P. Brueggeller, A. Romerosa, G. Sava and A. Bergamo, *Chem. Commun.*, 2003, 264–265.

4 (*a*) C. S. Allardyce, P. J. Dyson, D. J. Ellis and S. L. Heath, *Chem. Commun.*, 2001, 1396–1397; (*b*) C. Scolaro, A. Bergamo, L. Brescacin, R. Delfino, M. Cocchietto, G. Laurenczy, T. J. Geldbach, G. Sava and P. J. Dyson, *J. Med. Chem.*, 2005, **48**, 4161–4171; (*c*) P. J. Dyson and G. Sava, *Dalton Trans.*, 2006, 1929–1933; (*d*) P. J. Dyson, *Chimia*, 2007, **61**, 698–703; (*e*) A. Bergamo, A. Masi, P. J. Dyson and G. Sava, *Internet J. Oncol.*, 2008, **33**, 1281–1289; (*f*) W. H. Ang, A. Casini, G. Sava and P. J. Dyson, *J. Organomet. Chem.*, 2011, **696**, 989–998; (*g*) C. M. Clavel, E. Paunescu, P. Nowak-Sliwinska, A. W. Griffioen, R. Scopelliti and P. J. Dyson, *J. Med. Chem.*, 2015, **58**, 3356–3365; (*h*) M. V. Babak, S. M. Meier, K. V. M. Huber, J. Reynisson, A. A. Legin, M. A. Jakupec, A. Roller, A. Stukalov, M. Gridling, K. L. Bennett, J. Colinge, W. Berger, P. J. Dyson, G. Superti-Furga, B. K. Keppler and C. G. Hartinger, *Chem. Sci.*, 2015, **6**, 2449–2456; (*i*) A. Weiss, X. Ding, J. R. van Beijnum, I. Wong, T. J. Wong, R. H. Berndsen, O. Dormond, M. Dallinga, L. Shen, R. O. Schlingemann, R. Pili, C.-M. Ho, P. J. Dyson, H. van den Bergh, A. W. Griffioen and P. Nowak-Sliwinska, *Angiogenesis*, 2015, **18**, 233–244; (*j*) B. S. Murray, M. V. Babak, C. G. Hartinger and P. J. Dyson, *Coord. Chem. Rev.*, 2016, **306**, 86–114.

5 (*a*) A. García-Fernández, J. Díez, Á. Manteca, J. Sánchez, R. García-Navas, B. G. Sierra, F. Mollinedo, M. Pilar Gamasa and E. Lastra, *Dalton Trans.*, 2010, **39**, 10186–10196; (*b*) E. Menéndez-Pedregal, J. Díez, Á. Manteca, J. Sánchez, A. C. Bento, R. García-Navas, F. Mollinedo, M. Pilar Gamasa and E. Lastra, *Dalton Trans.*, 2013, **42**, 13955–13967.

6 R. Pettinari, F. Marchetti, F. Condello, C. Pettinari, G. Lupidi, R. Scopelliti, S. Mukhopadhyay, T. Riedel and P. J. Dyson, *Organometallics*, 2014, **33**, 3709–3715.

7 A. Wołoszyn, C. Pettinari, R. Pettinari, G. V. Badillo Patzmay, A. Kwiecień, G. Lupidi, M. Nabissi, G. Santoni and P. Smoleński, *Dalton Trans.*, 2017, **46**, 10073–10081.

8 (*a*) D. J. Darensbourg, F. Joó, M. Kannisto, Á. Kathó and J. H. Reibenspies, *Organometallics*, 1992, **11**, 1990–1993; (*b*) D. J. Darensbourg, F. Joó, M. Kannisto, A. Kath, J. H. Reibenspies and D. J. Daigle, *Inorg. Chem.*, 1994, **13**, 200–208; (*c*) F. Joó, L. Nádasdi, J. Elek and G. Laurenczy, *Chem. Commun.*, 1999, 971–972; (*d*) G. Laurenczy, F. Joó and L. Nádasdi, *Inorg. Chem.*, 2000, **39**, 5083–5088; (*e*) G. Laurenczy, F. Joó and L. Nádasdi, *High Pressure Res.*, 2000, **18**, 251–255; (*f*) G. Kovács, L. Nádasdi, G. Laurenczy and F. Joó, *Green Chem.*, 2003, **5**, 213–217.

9 *Aqueous-phase Organometallic Catalysis: Concepts and Applications*, ed. B. Cornils and W. A. Hermann, Wiley-VCH, Weinheim, 2nd edn, 2004.

10 W.-C. Lee and B. J. Frost, *Green Chem.*, 2012, **14**, 62–66.

11 F. Battistin, A. Vidal, P. Cavigli, G. Balducci, E. Iengo and E. Alessio, *Inorg. Chem.*, 2020, **59**, 4068–4079 and references therein.

12 B. Serli, E. Zangrando, T. Gianferrara, C. Scolaro, P. J. Dyson, A. Bergamo and E. Alessio, *Eur. J. Inorg. Chem.*, 2005, 3423–3434.

13 A. Udvardy, A. C. Bényei and Á. Kathó, *J. Organomet. Chem.*, 2012, **717**, 116–122.

14 F. Battistin, G. Balducci, E. Iengo, N. Demitri and E. Alessio, *Eur. J. Inorg. Chem.*, 2016, 2850–2860.

15 F. Battistin, G. Balducci, B. Milani and E. Alessio, *Inorg. Chem.*, 2018, **57**, 6991–7005.

16 (*a*) F. Battistin, G. Balducci, N. Demitri, E. Iengo, B. Milani and E. Alessio, *Dalton Trans.*, 2015, **44**, 15671–15682; (*b*) F. Battistin, D. Siegmund, G. Balducci, E. Alessio and N. Metzler-Nolte, *Dalton Trans.*, 2019, **48**, 400–414.

17 In all the Ru(II) compounds described in this paper PTA is always bonded exclusively through the P atom , thus κP is omitted in the formulas.

18 G. Laurenczy, S. Jedner, E. Alessio and P. J. Dyson, *Inorg. Chem. Commun.*, 2007, **10**, 558–562.

19 P. Crochet and V. Cadierno, *Dalton Trans.*, 2014, **43**, 12447–12462.

20 S. Moret, P. J. Dyson and G. Laurenczy, *Nat. Commun.*, 2014, **5**, 4017–4024.

21 A. Guerriero, H. Bricout, K. Sordakis, M. Peruzzini, E. Monflier, F. Hapiot, G. Laurenczy and L. Gonsalvi, *ACS Catal.*, 2014, **4**, 3002–3012.

22 A. Guerriero, H. Bricout, M. Peruzzini, P. J. Dyson, E. Monflier, F. Hapiot, L. Gonsalvi and G. Laurenczy, *Inorg. Chim. Acta*, 2015, **431**, 132–138.

23 F. Scalambra, M. Serrano-Ruiz and A. Romerosa, *Dalton Trans.*, 2017, **46**, 5864–5871.

24 A. Udvardy, M. Serrano-Ruiz, V. Passarelli, E. Bolyog-Nagy, F. Joó, Á. Kathó and A. Romerosa, *Inorg. Chim. Acta*, 2018, **470**, 82–92.

25 T. R. Johnson, B. E. Mann, J. E. Clark, R. Foresti, C. J. Green and R. Motterlini, *Angew. Chem., Int. Ed.*, 2003, **42**, 3722–3729.

26 R. Motterlini and L. E. Otterbein, *Nat. Rev. Drug Discovery*, 2010, **9**, 728–743.

27 B. E. Mann, *Organometallics*, 2012, **31**, 5728–5735.

28 C. C. Romao, W. A. Blättler, J. D. Seixas and G. J. L. Bernardes, *Chem. Soc. Rev.*, 2012, **41**, 3571–3583.

29 S. H. Heinemann, T. Hoshi, M. Westerhausen and A. Schiller, *Chem. Commun.*, 2014, **50**, 3644–3660.

30 S. Garcia-Gallego and G. J. L. Bernardes, *Angew. Chem., Int. Ed.*, 2014, **53**, 9712–9721.

31 I. Chakraborty, S. J. Carrington and P. K. Mascharak, *Acc. Chem. Res.*, 2014, **47**, 2603–2611.

32 U. Schatzschneider, *Br. J. Pharmacol.*, 2015, **172**, 1638–1650.

33 J. Marhenke, L. Trevino and C. Works, *Coord. Chem. Rev.*, 2016, **306**, 533–543.

34 M. A. Wright and J. A. Wright, *Dalton Trans.*, 2016, **45**, 6801–6811.

35 M. Kubeil, R. R. Vernooij, C. Kubeil, B. R. Wood, B. Graham, H. Stephan and L. Spiccia, *Inorg. Chem.*, 2017, **56**, 5941–5952.

36 S. Bolaño, J. Bravo, J. Castro, M. M. Rodríguez-Rocha, M. F. C. Guedes da Silva, A. J. L. Pombeiro, L. Gonsalvi and M. Peruzzini, *Eur. J. Inorg. Chem.*, 2007, 5523–5532.

37 A. García-Fernández, J. Díez, A. Manteca, J. Sánchez, M. P. Gamasa and E. Lastra, *Polyhedron*, 2008, **27**, 1214–1228.

38 S. Bolaño, M. M. Rodriguez-Rocha, J. Bravo, J. Castro, E. Oñate and M. Peruzzini, *Organometallics*, 2009, **28**, 6020–6030.

39 S. Miguel, J. Díez, M. P. Gamasa and M. E. Lastra, *Eur. J. Inorg. Chem.*, 2011, **951**, 4745–4755.

40 A. García-Fernández, J. Díez, M. Pilar Gamasa and E. Lastra, *Eur. J. Inorg. Chem.*, 2014, **5**, 917–924.

41 L. Hajji, C. Saraiba-Bello, G. Segovia-Torrente, F. Scalambra and A. Romerosa, *Eur. J. Inorg. Chem.*, 2019, 4078–4086.

42 (*a*) F. Scalambra, M. Serrano-Ruiz, S. Nahim-Granados and A. Romerosa, *Eur. J. Inorg. Chem.*, 2016, 1528–1540; (*b*) F. Scalambra, N. Holzmann, L. Bernasconi, S. Imberti and A. Romerosa, *Eur. J. Inorg. Chem.*, 2019, 1162–1170.

43 E. Iengo, N. Demitri, G. Balducci and E. Alessio, *Dalton Trans.*, 2014, **43**, 12160–12163.

44 In the proton NMR spectrum of raw **10** a set of very small resonances, partially overlapped with those of **10**, presumably belonging to **11** (or perhaps to the corresponding complex with protonated PTA and thus more soluble) is barely visible. **11** could also be the product of a slow transformation of **10** (perhaps light mediated), since it forms in few weeks ESI.†

45 I. Bratsos, S. Calmo, E. Zangrando, G. Balducci and E. Alessio, *Inorg. Chem.*, 2013, **52**, 12120–12130.

46 C. F. J. Barnard, J. A. Daniels, J. Jeffery and R. J. Mawby, *Dalton Trans.*, 1976, 953–961.

47 (*a*) L. M. Wilkes, J. H. Nelson, J. P. Mitchener, M. W. Babich, W. C. Riley, B. J. Helland, R. A. Jacobson, M. Y. Cheng, L. Seff and L. B. McCusker, *Inorg. Chem.*, 1982, **21**, 1376–1382; (*b*) D. W. Krassowski, J. H. Nelson, K. R. Brower, D. Hauenstein and R. A. Jacobson, *Inorg. Chem.*, 1988, **27**, 4294–4301.

48 C. A. Mebi and B. J. Frost, *Inorg. Chem.*, 2007, **46**, 7115–7120.

49 R. Girotti, A. Romerosa, S. Mañas, M. Serrano-Rui and R. N. Perutz, *Inorg. Chem.*, 2009, **48**, 3692–3698.

50 J. Kovács, F. Joó, A. Bényei and G. Laurenzy, *Dalton Trans.*, 2004, 2336–2340.

51 F. Battistin, F. Scaletti, G. Balducci, S. Pillozzi, A. Arcangeli, L. Messori and E. Alessio, *J. Inorg. Biochem.*, 2016, **160**, 180–188.

52 D. N. Akbayeva, S. Moneti, M. Peruzzini, L. Gonsalvi, A. Ienco and F. Vizza, *C. R. Chim.*, 2005, **8**, 1491–1496.

53 S. Grguric-Sipka, C. R. Kowol, S.-M. Valiahdi, R. Eichinger, M. A. Jakupec, A. Roller, S. Shova, V. B. Arion and B. K. Keppler, *Eur. J. Inorg. Chem.*, 2007, 2870–2878.

54 S. Yazdani, B. E. Silva, T. C. Cao, A. L. Rheingold and D. B. Grotjahn, *Polyhedron*, 2018, **161**, 63–70.

55 L. Leyva, C. Sirlin, L. Rubio, C. Franco, R. Le Lagadec, J. Spencer, P. Bischoff, C. Gaiddon, J.-P. Loeffler and M. Pfeffer, *Eur. J. Inorg. Chem.*, 2007, 3055–3066.

56 F. Battistin, G. Balducci, J. Wei, A. K. Renfrew and E. Alessio, *Eur. J. Inorg. Chem.*, 2018, **2018**, 1469–1480.

57 W. Kabsch, *Acta Crystallogr., Sect. D: Biol. Crystallogr.*, 2010, **66**, 125–132.

58 G. M. Sheldrick, *Acta Crystallogr., Sect. A: Found. Adv.*, 2015, **72**, 3–8.

59 G. M. Sheldrick, *Acta Crystallogr., Sect. A: Found. Crystallogr.*, 2008, **64**, 112–122.

60 P. Emsley and K. Cowtan, *Acta Crystallogr., Sect. D: Biol. Crystallogr.*, 2004, **60**, 2126–2132.